SICE Transaction on Industrial Application
Vol. 9, No. 20, 148/155 (2010)

A Continuous Control Input Generation Method in Model Predictive Control for an Electromechanical Valve

Addy WAHYUDIE *, Taizo NAKAO **, Toshimitsu KAI *, Hideaki SETOGUCHI *
Masakazu MUKAI *, and Taketoshi KAWABE *

Abstract: This paper proposes a continuous control input generation method in model predictive control for an electromechanical valve. In previous works, the model predictive control generates a discontinuous control current for the valve actuation. From a practical point of view, it is difficult for an amplifier to generate a discontinuous current. A plant of the electromechanical valve is augmented with an integrator to generate continuous control input. A traveling time of the valve armature can be shortened by adjusting parameters of a state weighting matrix in a performance index of the model predictive control algorithm. In addition, the proposed method has an important feature that it is a deadbeat controller with a designed terminal condition of the valve armature. Therefore, the armature reaches a target position and velocity. The controller calculates the continuous optimum control in each sampling instant. A disturbance observer is used for estimating the armature velocity and improving robustness of the controlled system against parameter uncertainty. The proposed method is validated in computer simulation and experimental results.

Key Words: electromechanical valve, model predictive control, motion control, robust control

1. Introduction

Significant improvements in internal combustion engine can be achieved using the electromechanical valve (EMV) system [1]. The EMV system affords the valve timings that are fully independent of a crank-shanks position. Fuel saving (20% or higher) can be obtained by controlling the intake process at part load, eliminating intake air throttling and pumping losses. Pollutant emission reduction (NO_x and CO_x) is achieved by the possibility of achieving the high internal Exhaust Gas Recirculation (EGR) rate through both retarding and advancing the exhaust valve closing, resulting NO_x reduction up to 90%. Increasing of 10% in the maximum torque and up to 50% at the low speed torque are produced by optimizing the valve timing at all operating conditions, avoiding the compromise of mechanically driven camshafts.

A configuration of the EMV system is shown in **Fig. 1**. The EMV is driven by two electromagnets, two springs, and an armature. The armature travels between the two electromagnets. The armature is suspended by the two springs with large spring constant, enabling it to move at high speed. The springs are attached to make the armature balanced at the neutral position. In "open valve" operation, current at the upper-side electromagnet is switched off, and the armature moves to the lower electromagnet by the spring force. When the armature moves close to the lower electromagnet, the current is switched on to this electromagnet, so that pulling control force is available. For "close valve" operation, the electromagnets system works conversely.

In an actual application, the armature moves within a short distance (8–9 [mm]) over a short period of time (approximately 3–4 [ms]) [2, 3]. This short period of time is desirable in order to meet the maximum engine speed (5000 – 6000 [rpm]). Furthermore, a high speed collision between the armature and the electromagnet is not desirable. Some authors in [2–4] proposed that the impact velocity should be controlled in less than 0.1 [m/s] for maintaining the acceptable engine acoustic noise level, and for avoiding the valve is distorted by mechanical shock. To overcome the problems, motion of the armature is controlled by controlling the current in the pulling electromagnet. However, there are difficulties for controlling motion of the armature, such as:

1. The control input should be calculated in a very short period of time.
2. The pushing and pulling force are only available from the springs and the electromagnets, respectively. However, the pushing force cannot be controlled because it generated by the springs.
3. The magnetic force is effective only when the armature is very close to the pulling electromagnet.

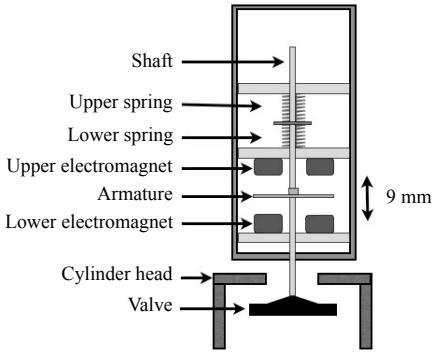

Fig. 1 Configuration of an electromechanical valve

* Graduate School of Information Science and Electrical Engineering, Kyushu University, Fukuoka, Japan.
** Nippon Steel Engineering Corp., Kitakyushu, Japan.

(Received June 16, 2010)

4. Nonlinearity of the electromagnet is large when the armature close to the electromagnets.
5. The valve should be opened/closed within the specified time in synchronization with the engine revolution.
6. There exist a delay of the electromagnet current.

The control method for the EMV systems have been studied in recent years. Most of these existed control method (for example papers [2–6]) showed that the armature is asymptotically converge to its desired position and velocity. The papers [7–8] used a iterative learning method for controlling the EMV. However, results showed that many learning processes are needed before achieving the armature achieving sufficient performance.

This paper apply an online deadbeat controller for controlling the armature motion using model predictive control (MPC) [9]. In this paper, the proposed method is expected to overcome the first five difficulties for controlling the EMV. In this paper, an improvement concerning a continuous control input generation for the EMV is proposed in this paper. In previous works [10–11], the MPC (so called the conventional MPC here) generates a discontinuous optimal control for the EMV. Although satisfactory results in the computer simulation and the experiment using a laboratory scale testbed are shown using the conventional MPC [12], it is difficult for an amplifier to generate a discontinuous input in an actual application. This because a lower quality of an amplifier is used in actual application. In order to provide the continuous control input for the EMV, the input is integrated using an integrator. The addition of the integrator in front of the EMV plant tends to yield a longer traveling time of the armature. However, the paper [13] showed that the traveling time in the proposed method can be shortened close to the traveling time in the conventional MPC by adjusting parameters of a state weighting matrix in a performance index of the MPC.

This paper is organized as follows. A model for the augmented plant of the EMV and the proposed controller design are describe in Section 2. Computer simulation results of the proposed controller for controlling an actual EMV, are given in Section 3. The proposed method is implemented on an experimental testbed. Experimental results using the proposed controller for the testbed are presented in Section 4. Finally, conclusions are given in Section 5.

2. Modeling and Controller Design

First, the MPC algorithm for a linear plant is proposed. Subsequently, a model of the EMV system is described. The proposed MPC algorithm is applied to the EMV system.

2.1 MPC for a Linear Plant

In this section, the MPC method for a linear plant is described. The linear plant has a state equation in form of

$$\dot{x}(t) = Ax(t) + Bu(t). \tag{1}$$

A and B are $n \times n$ system matrix and $n \times r$ input matrix, respectively. Here, $x(t) \in \mathbb{R}^n$ is state vector of the plant and $u(t) \in \mathbb{R}^m$ is the plant input. Standard iterative calculation methods are not used for calculation the optimal control in the MPC because it takes higher computation cost. The following procedure is proposed for calculating the optimal control. Differential equations are obtained from the procedure.

Let us consider the following performance index

$$J(\tau) = \frac{1}{2}\int_t^{t_f} \left(x(\tau)^T Q x(\tau) + u(\tau)^T R u(\tau) \right) d\tau, \tag{2}$$

subject to the state equation of linear plant in (1). Here, τ is virtual time for predictive control. t is the present time of the predictive horizon and t_f is the terminal time of the predictive horizon. The weighting matrix Q and R are real, constant, symmetric positive semi-definite and positive definite matrix, respectively.

The costate equation and the optimal input for (1) are stated as follows:

$$\dot{\lambda}(t) = -A^T\lambda(t) - Qx(t), \tag{3}$$

$$u(t) = -R^{-1}B^T\lambda(t). \tag{4}$$

Costate equation in (3) involves Lagrange multipliers λ that help us to find the optimal input by converting the constrained minimization problem into an unconstrained minimization problem. The optimal input is obtained by the following procedure.

Using the state equation (1) and the optimal input (4), we get

$$\dot{x}(t) = Ax(t) - BR^{-1}B^T\lambda(t). \tag{5}$$

Combining the equations (3) and (5) yield

$$\begin{bmatrix} \dot{x}(t) \\ \dot{\lambda}(t) \end{bmatrix} = \begin{bmatrix} A & -BR^{-1}B^T \\ -Q & -A^T \end{bmatrix} \begin{bmatrix} x(t) \\ \lambda(t) \end{bmatrix} = H \begin{bmatrix} x(t) \\ \lambda(t) \end{bmatrix}. \tag{6}$$

The general solution of the state equation the optimal input (6) at τ, given a initial condition at t is

$$\begin{bmatrix} x(\tau) \\ \lambda(\tau) \end{bmatrix} = e^{H(\tau - t)} \begin{bmatrix} x(t) \\ \lambda(t) \end{bmatrix}. \tag{7}$$

The transition matrix $e^{H(\tau-t)}$ is partitioned into

$$e^{H(\tau-t)} = \left[\begin{array}{c|c} e_{11}(\tau) & e_{12}(\tau) \\ \hline e_{21}(\tau) & e_{22}(\tau) \end{array}\right], \quad e_{11}(\tau), e_{22}(\tau) \in \mathbb{R}^{n\times n},$$

Evaluating (7) at t_f given initial condition at t obtains

$$x(t_f) = e_{11}(t_f)x(t) + e_{12}(t_f)\lambda(t),$$
$$\lambda(t) = e_{12}(t_f)^{-1}\left(x(t_f) - e_{11}(t_f)x(t)\right).$$

Evaluating (7) at τ by using $\lambda(t)$ yields

$$\lambda(\tau) = e_{21}(t)x(t) + e_{22}(\tau)e_{12}(t_f)^{-1}\left(x(t_f) - e_{11}(t_f)x(t)\right).$$

Using $\lambda(\tau)$ in the last equation, the optimal $u(\tau)$ can be obtained by using the following relationship

$$u(t) = -R^{-1}B^T\lambda(\tau),\ u(t) = u(\tau),\ \text{for } t \le \tau \le t + \Delta t,$$

where Δt is the sampling period of the MPC. The inverse of R is exist because R is positive definite matrix. Kalman [14] has shown that the inverse of e_{12} is exist for all $\tau \in [t, t_f]$. Therefore, the optimal $u(\tau)$ is exist.

In the MPC framework for the linear plant, the states variables are updated in each sampling instant. The MPC calculates the optimal $u(\tau)$ for the entire predictive horizon in each sampling instant. The predictive horizon is becoming shorter as time passing. The flowchart in **Fig. 2** summarizes the algorithm of the proposed MPC.

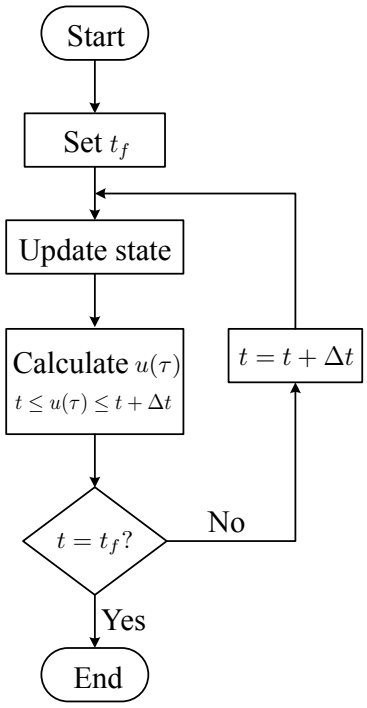

Fig. 2 Flowchart of the proposed MPC

2.2 Modeling

The EMV consists of an armature, two springs, a shaft, and a valve. The armature, shaft and valve are considered as one body, and called the moving part. The moving part has a mass m. It is suspended by the springs which have the spring constant k. The damping coefficient of the moving parts is c. Under those conditions, a motion equation of the moving part can be expressed as

$$m\ddot{z}(t) + c\dot{z}(t) + kz(t) = w(t) + d(t), \tag{8}$$

where w and d are the magnetic force and the external disturbance force, respectively. The moving part travels between $[-z_s,\ z_f]$. Here, z_s and z_f denote the surface position of the upper and the lower electromagnet, respectively. $z = 0$ is the neutral position.

We form an augmented plant for the EMV, by appending the EMV plant (8) with an integrator. The augmented plant for the EMV can be formulated in the state space equation as follows:

$$\dot{x}(t) = Ax(t) + B(u(t) + d(t)), \tag{9}$$

$$x(t) = \begin{bmatrix} w(t) \\ z(t) \\ \dot{z}(t) \end{bmatrix},\ A = \begin{bmatrix} 0 & 0 & 0 \\ 0 & 0 & 1 \\ \frac{1}{m} & -\frac{k}{m} & -\frac{c}{m} \end{bmatrix},\ B = \begin{bmatrix} 1 \\ 0 \\ 0 \end{bmatrix}.$$

The force w is converted to the electromagnetic current i by the following nonlinear equation

$$i = \sqrt{\frac{2w(l + k_2)^2}{k_1}}. \tag{10}$$

Here, l is the gap between the armature and the pulling magnet. The constants k_1 and k_2 are obtained through system identification [12]. Equation (10) represents the nonlinear property of the electromagnetic force in attracting the armature for various position of the armature and in various value of electromagnetic current. In this paper, delay of the electromagnet current in reaching its target value is neglected.

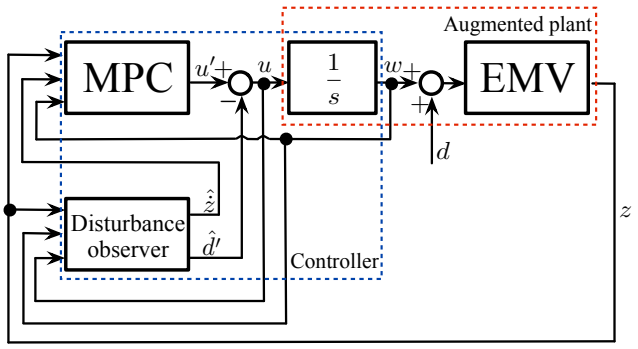

Fig. 3 Configuration of the proposed controlled system

2.3 MPC for an EMV

A configuration of the proposed controlled system is shown in **Fig. 3**. The optimal control force u' is calculated by the MPC compensator. The armature position and its velocity are needed for the calculation. The armature position z is obtained from direct measurement. The armature velocity $\hat{\dot{z}}$ is estimated using the disturbance observer. The controlled system robustness against parameter uncertainty is improved using the observer by sending the compensation force $\hat{d}'$. The control force u is obtained using u' and $\hat{d}'$. However, the discontinuous signal of u is tended to generate by the controller. In order to have the continuous control force w, the augmented plant of the EMV is formed by appending the EMV plant with the integrator. The discontinuous signal u is integrated by this integrator. In this paper, we assume that there is no external disturbance d.

The controller in **Fig. 3** mainly consists of two elements, i.e., the MPC compensator and the disturbance observer. These elements are described in the following sections.

2.3.1 MPC compensator

In this section, the MPC algorithm in Section 2.1 is applied to the EMV system for calculating u'. In ideal condition (there is no parameter perturbation), the compensation force $\hat{d}' = 0$ and thus $u = u'$. The performance index in (2) is used subject to the state equation of the augmented plant in (9), and positiveness of the control force w. The positiveness of w is required to assure that the armature is pulled to the desired electromagnet by the control force, because the electromagnet can only generate a pulling force.

In this paper, we consider an "open valve" operation. The initial state $x(t)$ and terminal state $x(t_f)$ are defined as

$$x(t) = [\ w_t\ \ z_t\ \ \dot{z}_t\ ]^T, \quad x(t_f) = \left[\ kz_f\ \ z_f\ \ 0\ \right]^T,$$

where w_t, z_t, $\dot{z}_t$ are present control force, present armature position, and present armature velocity, respectively. z_f is the desired position of the armature at terminal time (i.e., the position of the pulling electromagnet surface). The desired armature velocity is set to 0. The final force is determined so that kz_f and pulling force of the springs at surface of the electromagnet is balance. The weighting matrix Q is formulated as

$$Q = \begin{bmatrix} q_1 & 0 & 0 \\ 0 & q_2 & 0 \\ 0 & 0 & q_3 \end{bmatrix}.$$

In the MPC framework for the EMV, the variables w_t, z_t, $\dot{z}_t$, and t are updated in each sampling instant, while w_f, z_f and t_f

are fixed in all sampling instant. Furthermore, t_f is a designed traveling time of the armature.

Now, the positiveness of w is considered. From the result of numerical simulation in **Fig. 4**, important facts are observed that: a short traveling time makes the w negative between t_0 and t_f, and a long traveling time makes the w positive between t_0 and t_f. t_0 is the time when MPC start to work. According to the relationship, the following physical interpretation is also obtained. A short traveling time requires relatively a large force to slow down the armature velocity and place it to the desired final position, comparing to the case of long traveling time.

A shorter t_f needs a sudden acceleration and a sudden deceleration of the armature. This sudden deceleration leads to a negative w for the armature. A longer t_f admits a more moderate acceleration and a more moderate deceleration of the armature. This moderate deceleration force allows w still positive. Although w always positive for a sufficiently large t_f, the smallest t_f is selected to meet the maximum engine speed. The choice of t_f also consider limitation of the force that can be produced by the pulling electromagnet. For implementation, the admissible value of t_f that meets those requirements, can be obtained through computer simulation.

2.3.2 Disturbance observer

The disturbance observer in **Fig. 3** is used to estimate the armature velocity $\hat{\dot{z}}$. The disturbance observer is also used to compensate the perturbation of m, c, k and influence of the disturbance d in low frequency band. A structure of the disturbance observer for the EMV system is simply constructed by appending the compensation force $\hat{d}'$ to the state vector in (9) and augmenting the corresponding row in the state matrix with zeroes:

$$\hat{x}(t)' = (A' - LC')\hat{x}(t)' + Ly + B'u(t).$$

$$A' = \begin{bmatrix} A & B \\ 0 & 0 \end{bmatrix}, \quad B' = \begin{bmatrix} B \\ 0 \end{bmatrix}, \quad C' = [\,0\ 1\ 0\ 0\,],$$

$$x'(t) = [\ w(t)\ \ z(t)\ \ \dot{z}(t)\ \ d'(t)\ ]^T, \quad y(t) = C'x(t)'.$$

The observer gain L is designed by using a pole placement procedure. An appropriate L is chosen so that $(A' - LC')$ has stable eigenvalues, and the respond of the observer is faster than the response of the MPC.

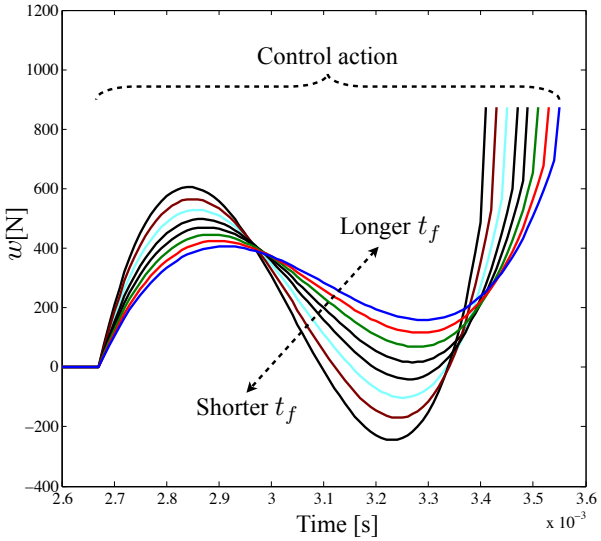

Fig. 4 The relationship between w and t_f

Table 1 Parameters of an actual EMV and its simulation setup

Parameter	Value	Unit
Sampling time of the MPC	4×10^{-5}	sec
Mass (m)	0.215	Kg
Spring constant, k	20×10^4	N/m
Viscous constant, c	12	N.sec/m
Upper magnet position, $-z_s$	−4.375	mm
Target position, z_f	4.375	mm
z when the MPC is started	3.375	mm
z when the MPC is terminated	4.3745	mm

3. Simulation Results Using an Actual EMV Parameters

In this section, computer simulations are conducted to control the EMV with its actual parameters (true industrial specifications) using the proposed method. The computer simulations show the effectiveness of the proposed method to overcome the first five problems in the difficulties for controlling motion of the armature. The parameters of actual EMV [2] and the simulation setup, are listed in **Table 1**. In the table, we use 5×10^{-5} [s] for the MPC sampling time . This sampling time is small enough for controlling the armature and have been successfully used in [5] for implementation of its online control law using a sophisticated control board. Therefore, the sampling time is considered to be available. Motion of the armature is controlled by controlling the current in the pulling electromagnet because we cannot controlled the spring force. The armature motion can only be controlled while it is closer than one millimeter from the pulling electromagnet, due to limitation of maximum current in the electromagnet. The nonlinearity of the electromagnet can be compensated using the nonlinear equation in (10). When the armature reaches a very close position from the pulling magnet, the MPC control action is terminated and the holding force is applied to keep armature on the magnet surface. The observer gain L is designed so that the eigenvalues of $(A' - LC')$ equal $-2\pi p \times 90$, $-2\pi p \times 90.1$, $-2\pi p \times 90.2$, and $-2\pi p \times 90.3$, where $p = \sqrt{k/m}$. Computer simulations are conducted using the proposed method and the conventional

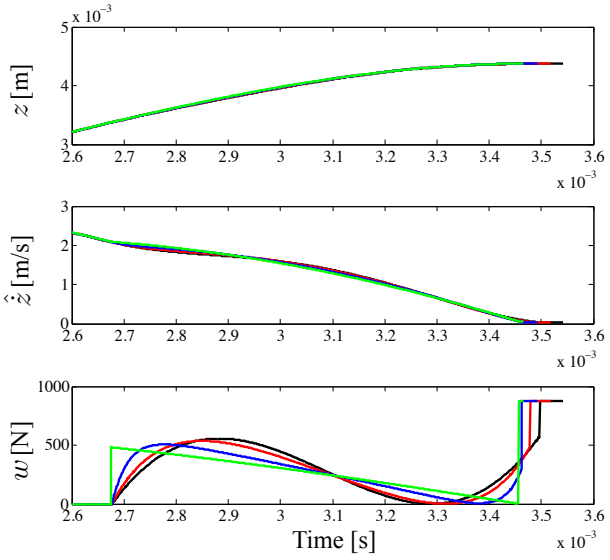

Fig. 5 Computer simulation results of the EMV with actual parameter using the conventional MPC method (green) and the proposed method with $q_1 = 0$ (black), $q_1 = 1 \times 10^8$ (red), and $q_1 = 1 \times 10^9$ (blue)

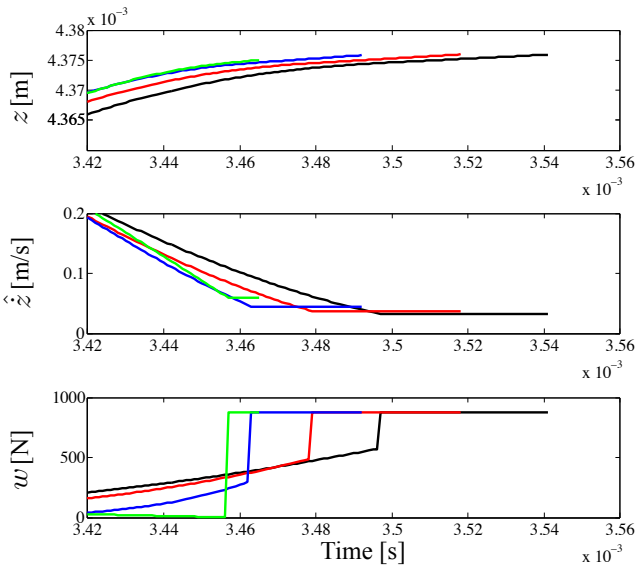

Fig. 6 Zoomed computer simulation results of **Fig. 5** at its final traveling time

MPC method [12]. The parameter q_2 and q_3 in the matrix Q are set to 0, while q_1 is varied. The weighting matrix R is set to 1. The simulation result is shown in **Fig. 5** and its zoomed computer simulation results at its final traveling time is shown in **Fig. 6**. The conventional MPC gives the minimum traveling time of the armature, compared to the one using the proposed method. The shorter t_f of the proposed method can be obtained by adjusting the value of q_1. The corresponding traveling time in **Fig. 5** is listed in **Table 2**.

Computer simulations are conducted for perturbed EMV model using the proposed method with $q_1 = 1 \times 10^9$ to evaluate robustness of the controlled system. In practical, there are perturbations in spring constant because of inaccuracy in spring machining. Perturbations in mass are unlikely to be happened. Influence of the viscous constant perturbations is small, owing

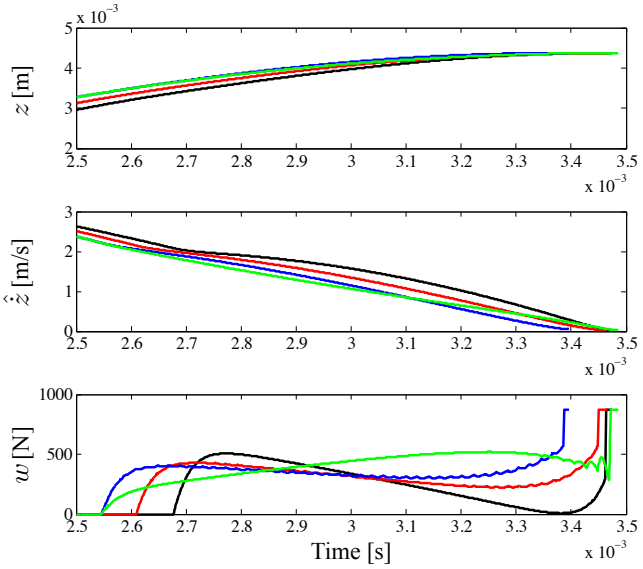

Fig. 7 Computer simulation results of the EMV with the actual parameters for nominal case (black), 5% perturbation of the k value (red), 10% perturbation of the k value (blue) using the proposed method, and 10% perturbation of the k value without using the compensation force (green)

Table 2 Comparison of the traveling time in **Fig. 5**

Method	Traveling time [s]
$q_1 = 0$	3.540×10^{-3}
$q_1 = 1 \times 10^8$	3.517×10^{-3}
$q_1 = 1 \times 10^9$	3.492×10^{-3}
Conventional MPC	3.473×10^{-3}

Table 3 The impact velocities in **Fig. 7** using the proposed method

Simulation case	$\hat{z}$ [m/s]
Nominal case	0.04
5% perturbation	0.03
10% perturbation	0.05

its relatively small value. Here, perturbations of spring constant are set at 5% and 10% larger than the nominal value. The simulation results are shown in **Fig. 7**. The control forces are kept continuously positive during the control action for the nominal case and perturbed ones by the proposed method. The armature traveling time is kept within the designed t_f, for the nominal case and its perturbations. The shape of w in perturbed cases are similar with the nominal case by using the disturbance observer. The impact velocities in **Fig. 7** are given in **Table 3**. All the impact velocities are less than 0.1 [m/s]. Since the armature can travel within its designed traveling time, this enables us to make synchronization with the timing of engine revolution and meets the required of maximum engine speed.

Therefore, the computer simulation results showed that the proposed method can overcome the first five difficulties for controlling motion of the armature. The proposed method enables low impact velocity for the armature and robustness of the controlled system is preserved

4. Experimental Results

A laboratory scale testbed is used for implementing the proposed method. The testbed is composed to study the principal properties of the proposed method such as the effectiveness of the proposed method for controlling the traveling time of the armature, providing low impact velocity, and low impact sound level. This testbed has different specifications compared with the actual EMV system that described in Section 3. Lower specifications or inexpensive parts/devices (i.e., electromagnets, power supply, control board, sensors) are used for the testbed. Due to the limitation of power supply that we can provide for controlling the testbed of EMV, a longer t_f is used in the experiments, compared with the t_f in Section 3. This longer t_f is implemented using a lighter mass of the armature and the springs with lower spring constant.

First, the experimental device setup for implementation of the proposed method on a testbed is described. Sequently, the experimental results using the testbed are showed.

4.1 Experimental Device Setup

The experimental device setup is shown in **Fig. 8**. Real-time implementation of the control law is coded in C using a dSPACE DS1104 control board. In each sampling instant, the control board reads the armature position as analog input, estimates the armature velocity, and calculates the control input. The control input from the control board is amplified using a LM3886 audio amplifier from National Semiconductor. A DC power supply is used for the audio amplifier that can generate ± 50 [V] / 5 [A]. The pulling force is provided by two par-

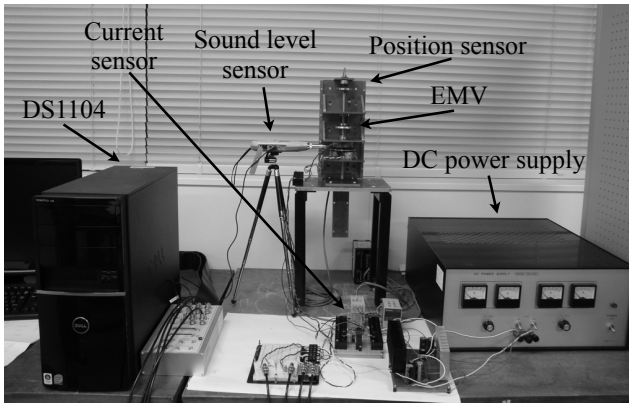

Fig. 8 The experimental device setup

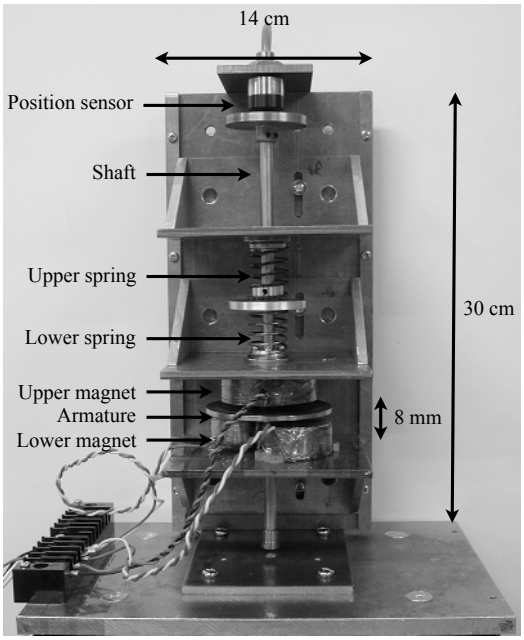

Fig. 9 The testbed of an electromechanical valve

Table 4 Parameters of the testbed and its experimental setup

Parameter	Value	Unit
Sampling time of the MPC	1.8×10^{-4}	sec
Mass m	0.285	Kg
Spring constant, k	1333.3	N/m
Viscous constant, c	1.6239	N.sec/m
k_1	3.59	N.mm^2/A^2
k_2	1.3379	N.mm^2/A^2
Q	0	–
Upper magnet position, $-z_s$	−4.300	mm
Target position, z_f	4.300	mm
z when MPC is started	3.300	mm
z when MPC is terminated	4.29	mm
Traveling time t_f	5.58×10^{-2}	sec

allel electromagnets. The armature displacement is measured by an inductive displacement sensor (Keyence EX-422V). A U.R.D. HCS-20-AP device is used as a current sensor. Impact sound level is measured using a precision sound level sensor (Rion N-15). The sound sensor is set to "A" weighting option, to give actual impression of loudness. Detail of the EMV testbed is shown in **Fig. 9**.

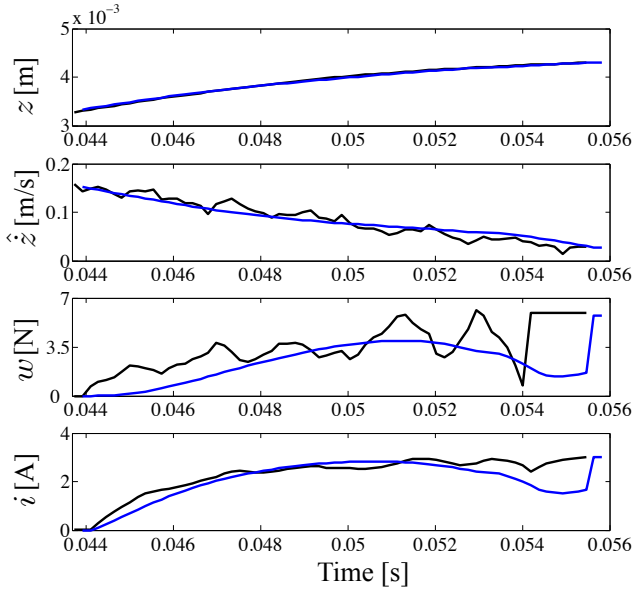

Fig. 10 Comparison of the measured (black) and simulated (blue) results using the proposed method

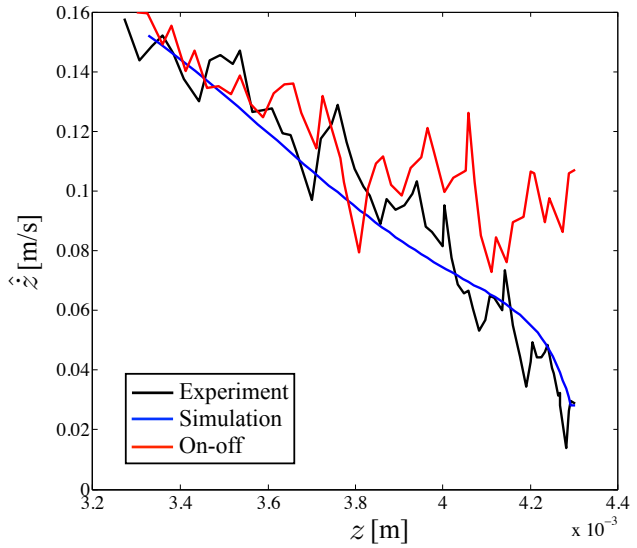

Fig. 11 Comparison of the experimental and computer simulation results in a phase plane

4.2 Experimental Results

In this section, effectiveness of the proposed method in controlling the armature of the EMV testbed is showed. The parameters of the testbed and its experimental setup are listed in **Table 4**. The system identification process for obtaining parameters m, c, k, k_1, k_2 are described in [12]. Similar with Section 3, the armature is controlled within the one millimeter from the pulling electromagnet. The experimental and simulated results for the testbed using the proposed method, are shown in **Fig. 10**. The experimental results are similar with its simulated results. The dSPACE DS1104 control board can calculate the control input of the MPC in each sampling time. A ripple control signal is appeared in w because of noise on z and $\hat{z}$ due to the noise of position sensor. Uncertainties of the model and delay of the current in reaching its target value are also become another source of the ripple control signal. In the experimental results, the target position is reached slightly faster than the de-

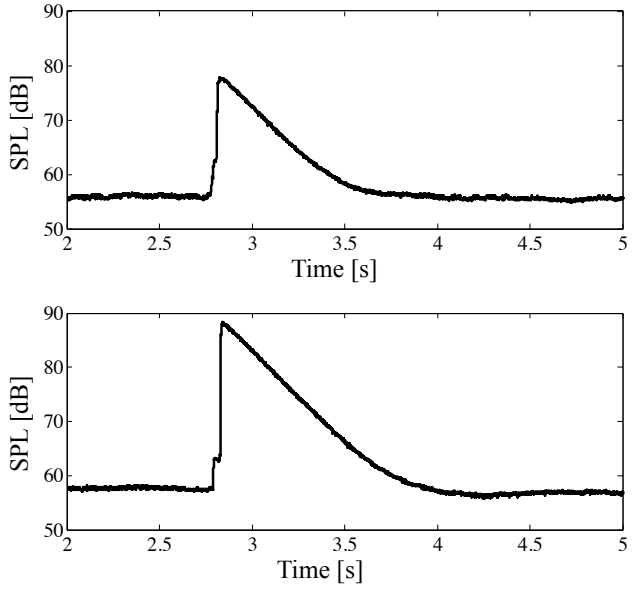

Fig. 12 Sound pressure level of the armature impact using the proposed method (upper), and the on-off control (lower)

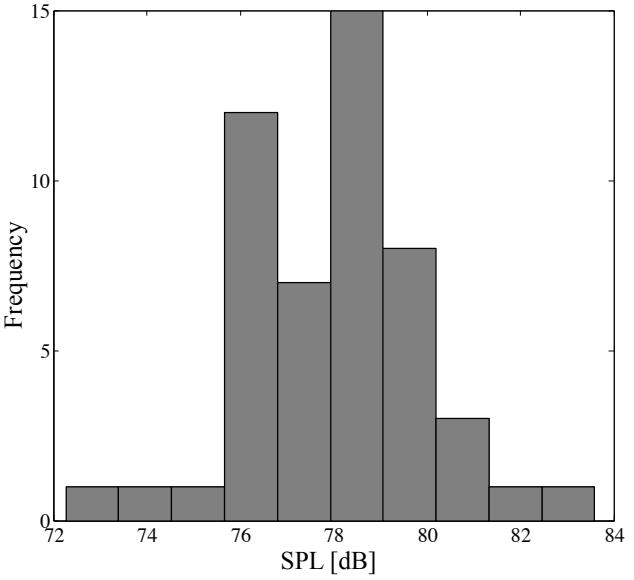

Fig. 13 Distribution of the sound pressure level for fifty experimental-cycles, using the proposed method

signed t_f. The t_f discrepancy because stopping condition of the MPC is influenced by noise of the position sensor.

Phase plane plots of the armature positions and its velocities are given in **Fig. 11**. The figure also shows experimental result when on-off control (i.e., the holding force is given to the lower electromagnets, when the armature reaches 1 [mm] from the desired position) is applied to the testbed. The phase plant plots show that the states in experimental result using the proposed method are converged to its simulated states within the designed t_f.

Effectiveness of the proposed method to reduce an impact sound level is shown in **Fig. 12**. A maximum Sound Pressure Level (SPL) of 77.92 [dB] and 85.6 [dB] are resulted by the proposed method and the on-off control, respectively. This result also indicates effectiveness of the proposed method to provide a low impact velocity. Fifty experimental-cycles are conducted using the proposed method and its resulted impact sounds are measured. A low average of impact sound level (77.97 [dB]) and a small standard deviation (1.9 [dB]) are obtained, as shown in **Fig. 13**. The results show ability of the proposed method to repeatedly enable the low impact sound level. In average, a difference of loudness (7.63 [dB]) is obtained using the proposed method and the on-off control. Therefore, the proposed method can suppress the maximum value of the impact sound level by 7.63 [dB].

5. Conclusion

An continuous control input generation method in MPC for an EMV has been proposed. A set of differential equations have been derived for calculating the optimal control for the EMV. The simulation results for EMV using actual parameters have showed that the proposed method can overcome the first five difficulties for controlling the armature of EMV and has met the requirements in the actual application. In the computer simulation and the experimental results, the proposed method has been implemented successfully using relatively small sampling times of the MPC compared with their traveling times of the armature. Based on the experimental results, the proposed method has been proved successfully in handling the nonlinearity of the electromagnet force for controlling the testbed. The armature has reached desired states within the certain designed traveling time in the simulation and the experimental results. The proposed method has enabled the low impact velocity, while robustness against the uncertain parameter model has been preserved. The proposed method has effectively reduced the impact sound level. The ability of the proposed method for maintaining the low impact sound level in many cycles has been showed. Hence, it can be concluded that the proposed method gives satisfactory performances, despite the difficulties for controlling the EMV.

References

[1] M. Pischinger, W. Salber, F. van der Staay, H. Baumgarten, and H. Kemper: Benefits of the electromechanical valve train in vehicle operation, SAE, New York, *SAE 2000-01-1223* (2000)

[2] S. K. Chung, and C. K. Koch: Flatness-Based Feedback Control of an Automotive Solenoid Valve, *IEEE Journal of Cont. Sys. Technology*, Vol. 15, No. 2, pp. 394–401 (2007)

[3] Y. Wang, T. Megli, M. Haghgooie, K.S. Peterson, and A.G. Stefanopoulou: Modeling and Control of Electromechanical Valve Actuator, *SAE 2002-01-1106* (2002)

[4] M. Montanari, F. Rotchi, C. Rossi, and A. Tonielli: Control of Camless Engine Electromechanical Actuator: Position Reconstruction and Dynamic Performance Analysis, *IEEE Trans. on Industrial Electronics*, Vol. 51, No. 2, pp. 299–311 (2004)

[5] T. Kawabe: Initial condition-adaptive Robust Control for a High-speed Magnetic Actuator, *Control Engineering Practice*, Vol. 11, No. 6, pp. 675–685 (2003)

[6] M. Uchida, R. Murata, T. Yabumi, Y. Morita, and H. Kando: Sliding Mode Servo Control for Electromagnetic Engine Valve, *Proc. SICE-ICASE Int. Joint Conf. 2006*, pp. 3658–3663 (2006)

[7] W. Hofmann, K. Peterson, and A. G. Stefanopoulou: Iterative Learning Control for Soft landing of Electromechanical Valve Actuator in Camless Engine, *IEEE Trans. on Cont. Systems Tech.*, Vol. 11, No. 2, pp. 174–184 (2003)

[8] K. Peterson, and A. G. Stefanopoulou: Extremum Seeking Control for Soft Landing of an Electromechanical Valve Actuator, *Automatica*, Vol. 40, No. 6, pp. 1063–1069 (2004)

[9] J. M. Maciejowski: Predictive Control with Constraints, Pear-

son Education Limited (2002)
[10] M. Mukai, S. Seikoba, T. Kawabe: A Model Predictive Control Method for a High-speed Magnetic Actuator, *Proc. in Chinese Control Conference 2007*, pp. 623–626 (2007)
[11] M. Mukai, S. Seikoba, T. Kawabe: Output Feedback Model Predictive Control for an Electromechanical Valve Actuator, *Proc. in SICE Annual Conf. 2007*, pp. 1734–1738 (2007)
[12] A. Wahyudie, T. Nakao, T. Kai, S. Seikoba, M. Mukai, and T. Kawabe: Model Predictive Controller with Fixed Compensator for an Electromechanical Valve, *SICE Journal of Cont., Meas., and Sys. Integ.,*, Vol. 3, No. 5, pp. 381–387 (2010)
[13] T. Nakao, A. Wahyudie, M. Mukai, and T. Kawabe: An Input Modification in Model Predictive Control by using Augmented Plant, *Proc. in MOVIC 2009*, pp. 295–298 (2009)
[14] R. E. Kalman: Contributions to the Theory of Optimal Control, *Bol. Soc. Mat. Mex*, pp. 102–119 (1960)

Addy Wahyudie (Student Member)

He finished his B. Eng. in 2002 from Gadjah Mada University, and M. Eng. in 2005 from Chulalongkorn University. Currently, he is a Doctoral student in the Graduate School of Information Science and Electrical Engineering, Kyushu University. His research interests include robust optimal control theory and its applications.

Taizo Nakao

He received his B. E. and M.E. from the Department of Electrical Engineering, Kyushu University in 2008 and 2010, respectively. His research interests include receding horizon control and its applications in automotive control technology. He is currently with Nippon Steel Engineering Corp.

Toshimitsu Kai

He received his B. E. from the Department of Electrical Engineering, Kyushu University in 2009. Currently, he is a student in the master's in the Graduate School of Information Science and Electrical Engineering, Kyushu University. His research interests include receding horizon control and its applications.

Hideaki Setoguchi

He received his B. E., from the Department of Electrical Engineering, Kyushu University in 2010. Currently, He is a student in the master's degree in the Automotive Science Department, Kyushu University. His research interests include receding horizon control and its application on automotive control technology.

Masakazu Mukai (Member)

He received the B.E., M.E. and Dr. of Engineering degrees in Electrical Engineering from Kanazawa University, in 2000, 2002, and 2005, respectively. He is currently with the Graduate School of Information Science and Electrical Engineering, Kyushu University. His research interests include receding horizon control and its applications. He is a member of the ISCIE, IEEJ, and IEEE.

Taketoshi Kawabe (Member)

He received the B. Sc. degree from the Department of Applied Physics, School of Science and Engineering, Waseda University in 1981, and M. Sc. from the Major in Pure and Applied Physics, Waseda University in 1984. He had been working with Nissan Research Center, Nissan Motor Co., Ltd. since 1984 to 2005. He was a research student of the Department of Mathematical Engineering and Information Physics, the University of Tokyo in 1992 and 1993, and received the Ph. D degree from the University of Tokyo in 1994. He is currently a professor in the Faculty of Information Science and Electrical Engineering, Kyushu University since April 2005. His research interests include motion control, vibration control and related automotive control technology. He is a member of the JSME, IEEJ, Society of Automotive Engineering of Japan and IEEE.